ARTICLE

Structure-Based Color of Natural Petals Discriminated by Polymer Replication

Seung-Mo Lee,*,† Johannes Üpping,‡ Andreas Bielawny,‡ and Mato Knez*,†

Max Planck Institute of Microstructure Physics, Weinberg 2, D-06120 Halle, Germany, and Institute of Physics, MD group, Martin-Luther-University of Halle-Wittenberg, Heinrich-Damerow-Strasse 4, D-06120 Halle, Germany

ABSTRACT The optical appearance of many flowers in nature relies on their inherent pigments ("chemical color") as well as on the surface structure of the epidermis ("structural color"). The structural color is created by a combination of regular and irregular micro- and nanosized features. With a red rose petal as a biological template, we have separated the structural coloration from the chemical coloration by reproducing the petal's intricate surface structure in a pigment-free polymer. UV−vis reflectance measurements of the templates showed that the pigment-induced chemical coloration of the red-rose petal results in intense absorption and reflection in the green (~550 nm) and red (~700 nm) spectral region, respectively. The micro- and nanosized structural hierarchy on the petal surface, on the other hand, induced a modulation of the optical reflectivity and a filtering effect in specific wavelength ranges. More notably, we observed that a variation in the size of the micro/nanostructures on the petal surface leads to an effective modulation of the reflectance. These results could provide useful tips for the design of bioinspired optical devices, emulating natural petal structures.

KEYWORDS: polymer replica • structural color • bioinspired optical design • natural petal structure • atomic layer deposition

INTRODUCTION

In many flower petals, the surface structure of the epidermis shows a combination of regular and irregular micro- and nanosized substructures (1, 2). In spite of having been described about a century ago (3), those surface structures are still believed to mainly function as tactile stimuli for insect pollinators for surface recognition or as favorable structures to walk on (2). Only recently, another interesting function of those structures has been reported: Superhydrophobicity with a high sliding angle for water droplets (4). It has also been reported that the petal's surface can generate a structure-based coloration by diffraction (5, 6), which is similar to observations from fishes (7), birds (8, 9), plant leaves (10, 11), insects (12), and reptiles (13). Meanwhile, motivated by these findings, diverse surface structures of natural petals became inspiring media for biomimetic surfaces and materials (1, 14, 15). Here, we report on the peculiar optical properties of polymers, which were replicated from surface structures of natural petals, showing structure-induced coloration effects. We reproduced a red-rose (RR) petal structure in polydimethylsiloxane (PDMS) following a two-step template approach, initially electroforming the structure from nickel and subsequently replicating the inverse structure with the polymer. The optical properties of the PDMS replica and the native red-rose petal were characterized by UV−vis reflectivity measurements. The chemical coloration of the red-rose petals, induced by the pigments, mainly affects an intense absorption and reflection in the green (~550 nm) and red (~700 nm) spectral region, respectively. The hierarchical micro- and nanostructures of the replica surface, on the other hand, show a pronounced effect on the reflectivity of PDMS. Namely, the reflectivity was modulated and an optical filtering effect in a specific wavelength range appeared as a result of the introduction of a structural hierarchy. We also observed that the reflectance, which is a function of the size of the micro/nanostructures distributed on petal surface, can be tuned by changing the size of the structures (shifting the reflectance to a longer wavelength). These results could provide useful tips for the design of bioinspired optical devices emulating natural petal structures.

* Corresponding author. E-mail: smlee@mpi-halle.mpg.de (S.-M.L); mknez@mpi-halle.mpg.de (M.K.).

Received for review August 27, 2010 and accepted November 3, 2010

† Max Planck Institute of Microstructure Physics.

‡ Martin-Luther-University of Halle-Wittenberg.

DOI: 10.1021/am1007968

EXPERIMENTAL SECTION

Nickel Stamp. The dried biotemplates were carefully bonded to a 4 in. silicon wafer with an epoxy adhesive (Figure 1A). Gold coating (around 3−6 nm thick) of the biotemplates was performed with a sputter coater, conventionally used for scanning electron microscope (SEM) sample preparation (Figure 1B). Nickel electroforming (Figure 1C) was carried out under following processing conditions: Temperature of the electrolyte solution (composed of $Ni(SO_3NH_2)_2$, $NiCl_2•6H_2O$ and H_3BO_3) was 55 °C; the current density was 0.3−1.3 mA · dm^{-2}; the pH of the electrolyte solution was 4.1. Subsequently, the silicon, the adhesive, and the biotemplate were separated from the nickel stamp with a KOH solution (at 70 °C), resulting in a pure nickel stamp (Figure 1D). The SEM examinations of all samples were performed with a JEOL JSM-6340F and a FEI XL 30S microscope.

PDMS Thermal Molding (Figure 1E,F). A Sylgard (R) 184 silicone elastomer kit (Dow Corning) was used for the preparation of flat and patterned PDMS replica. The PDMS prepolymer and curing agent were mixed (weight ratio = 10:1). The mixture was diluted in hexane (40% weight ratio). A cleaned 4 in. silicon wafer or the nickel stamp was positioned onto a cleaned 4 in. Petri dish. The diluted PDMS mixture was poured into the dish and maintained still for around 30 min. The subsequent curing was carried out in an oven at 70 °C overnight and the replicas

Published on Web 11/16/2010

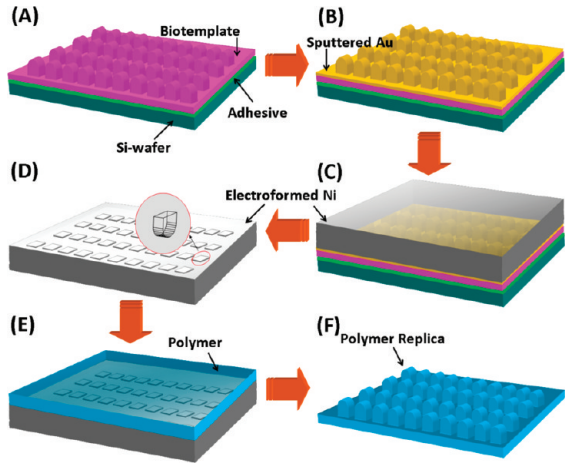

FIGURE 1. Schematic of the nickel stamp and the polymer replica preparation procedure. (A) Biotemplates are bonded by an adhesive to a silicon wafer. (B) Au layer is deposited on top (around 3−6 nm thick). (C) Nickel electroforming is carried out. (D) Electroformed nickel is separated from the substrates. (E, F) Preparation procedure for the polymer replica (in our case, PDMS molding).

were detached from the silicon wafer and the nickel stamp, respectively.

Al_2O_3 Atomic Layer Deposition (ALD). The red-rose petal was placed in an ALD reactor (Savannah 100, Cambridge Nanotech Inc.) and dried at 70 °C for 200 min in a vacuum (1×10^{-2} Torr) with a steady Ar gas stream (20 sccm). For the Al_2O_3 deposition, $Al(CH_3)_3$ (Sigma-Aldrich) and deionized H_2O were used as aluminum and oxygen sources, respectively. During the deposition process, the petals were alternately exposed/purged to/from $Al(CH_3)_3$ and H_2O vapor. The pulse/exposure/purge time of $Al(CH_3)_3$ and H_2O was 0.1/30/40 s and 1.5/30/40 s, respectively. The growth rate of the Al_2O_3 layer was about 1.0 Å per cycle. For the preparation of samples with differing thicknesses of Al_2O_3, the cycle number was changed from 100 to 300 and 500, respectively.

UV−Vis Reflectivity Measurement. The reflectivity of the samples in the spectral range of 370−725 nm has been measured with a fiber-coupled spectrometer on a BX51 optical microscope (Olympus) at normal incidence, along with capturing photographs in bright- and dark-field illumination. The used detector was a Hamamatsu S3904−256Q. The magnification was 50 times and the numerical aperture of the objective was 0.1. A polished Si wafer was used as reference. Before the measurements, all petal samples were flattened by keeping them between the leaves of a book for several days. Samples with sizes of around 15 mm by 15 mm were cut out with a pencil knife. In order to minimize the back-side reflection of the samples and the substrate signals, the smooth back-sides of the flat PDMS and the replicas were scratched using a sharp knife and sand paper. Subsequently, the roughened back-side surface was darkened with a black marker pen before the measurement. The samples were mounted on a black carbon tape supported on a silicon wafer (16). Under the microscope, well-defined and uniform areas of the samples were selected and the reflectivity of each sample was measured, including the reflectivity of the carbon tape itself. Subsequently, the reflectivity of the carbon tape was subtracted from the reflectivity of the samples. Each measurement was repeated several times on different locations. Most of the spectra showed very similar profiles. In the case of a native red-rose petal, the same procedure was applied, omitting the scratching step. For the representation, a typical spectrum was selected. All graphics jobs were done with the Origin 7.0 software.

RESULTS AND DISCUSSION

For the preparation of the polymer replicas from the surface structures of natural templates, initially, a mechanically durable nickel stamp was prepared by nickel electroforming (17). As depicted in Figure 1, the dried biotemplate was gently pressed on a silicon wafer and bonded by an adhesive (Figure 1A). Au (employed as an electrically conductive layer) with a thickness of 3−6 nm was deposited on top with an Au ion coater, conventionally used for SEM (scanning electron microscope) sample preparation (Figure 1B). Subsequently, nickel electroforming was carried out (Figure 1C). The nickel stamp (Figure 1D) served as negative master for the production of the polymer replicas. Such polymer replicas can in principle be obtained with diverse routine polymer processing techniques such as nanoimprint lithography, injection molding, and hot embossing. In this study, however, because of the simple processing procedure, we chose a simple thermal molding technique with PDMS (Figure 1E,F). Because PDMS has a low surface tension and very high viscosity, the replication quality of the nanosized structures may suffer, although microsized structures can be excellently replicated. Therefore, the PDMS was diluted in hexane, in order to enhance the structural fidelity of the PDMS replicas (See details in the Experimental Section) (18).

The efficiency of the described two-step process for obtaining polymer replica of the biotemplates was comparatively good. Figure 2 and Figure 3 show SEM images of examples of structures which were inverted by nickel electroforming and subsequently replicated in PDMS. In all four cases, that is, a moth wing (Figure 2A), a cicada wing (Figure 2B), a dragonfly wing (Figure 2C), and a red-rose petal (Figure 3), the polymer replicas exhibit generally a good replication quality, although slight size and structure discrepancies between the native structure and the replica were observed in some cases. These discrepancies are presumably caused by the sputtered Au layer. However, further factors, such as the chemistry of the nickel electrolyte solution and the molding technique itself, may also influence the structural features of the replica. For example, the used nickel electrolyte solution was acidic (pH 4.1). Because biotemplates are often sensitive to acids, during the initial stage of the nickel electroforming, the biotemplates could undergo partial decomposition by the electrolyte solution (19). Rose petals, on the other hand, are coated with a thin wax layer, protecting the petal from environmental influence. A degradation of the petal by the acidic electrolyte might be prevented by the wax during the initial stage of electroforming. Thus the discrepancy in the feature sizes might be rather a result of the sputtering than of the denaturation by acids. The PDMS replica produced from the prepared nickel stamps showed larger feature sizes, which may be another indication for the sputtering as source for the discrepancy. A degradation of the biomaterial would rather result in smaller feature sizes or loss of structural information. The molding technique and the type of the used polymer could be further factors contributing to the discrepancy, because each polymer processing technique shows different transcriptabilities, strongly relying on the process-

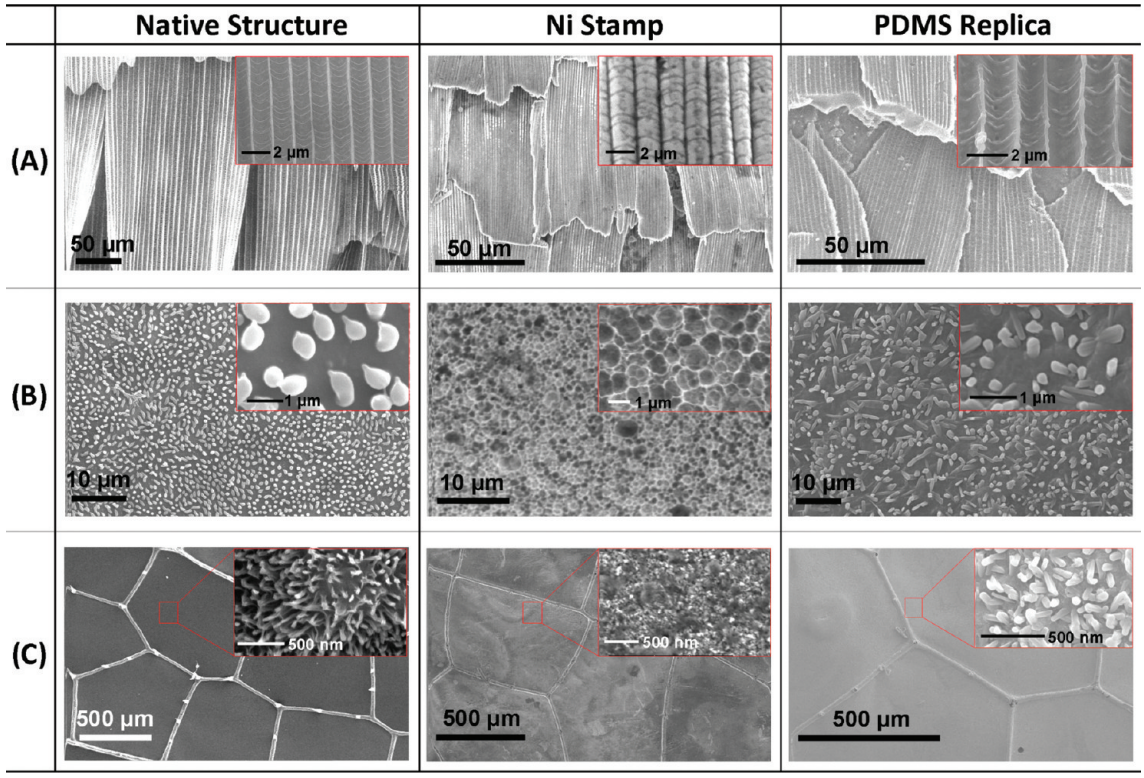

FIGURE 2. Further examples of biotemplates, negative nickel replicas, and positive PDMS replicas of (A) a moth wing, (B) a cicada wing, and (C) a dragonfly wing.

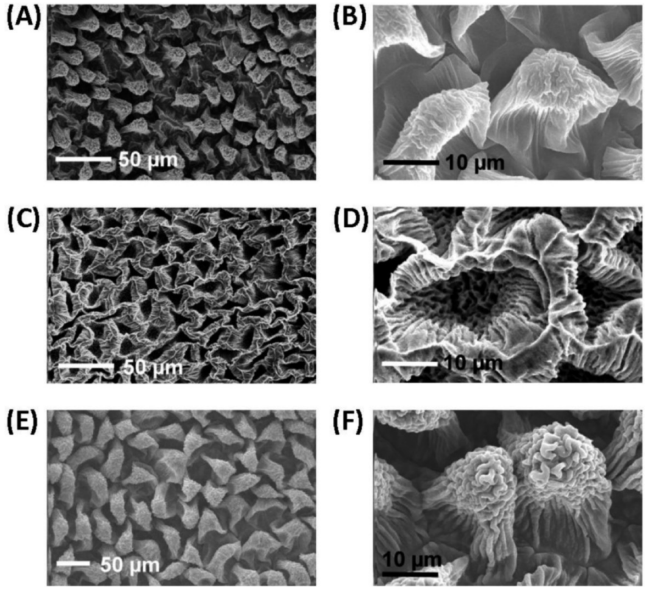

FIGURE 3. SEM images of an air-dried native red-rose petal surface (A, B), the nickel stamp with negative patterns of the red-rose petal (C, D), and the positive PDMS replica (E, F) in low- and high-magnifications, respectively.

ing conditions and the physical properties of the used polymers (such as the viscosity in a molten state). A reasonable selection of the nickel electrolyte solution and the molding technique could minimize these discrepancies, promising for general applicability. One drawback of the method is the sensitivity to surface features. This means that structures, which are buried below the surface, like in the scales of *Morpho* butterflies, can not be easily replicated or copied. Those structures require more sophisticated strategies which include, for example, atomic layer deposition (ALD) (16) or electroless deposition. Nevertheless, the electroforming approach promises replications of surface structures with feature sizes down to 20 nm, unless the structures are too branched (20, 21), which makes the strategy very attractive. For our investigations, we concentrated on a template that exhibits both a structure-based and a pigment-based color, with structural features confined to the uppermost part of the epidermis and showing no buried micro/nanostructures. A very simple and readily obtainable example of such a biotemplate is the rose petal.

Figure 3 shows SEM images of the surface structures of an air-dried native red-rose petal, a negative nickel replica and a positive PDMS replica, respectively. The SEM investigation of the air-dried native red-rose petal (Figures 3A,B) shows that micrometer-sized papilla patterns (in the order of tens of micrometers) are overlaid with sub-micrometer-sized ridges. However, unlike in the SEM investigations of red roses found in literature, the papilla patterns of the petal revealed shrunk forms. This is presumably due to the loss of water from the epidermal cells during the sample preparation, which apparently in our case was done more extensively than for the SEM sample preparation (2). Images C and D in Figure 3 indicate that the nickel stamp successfully replicates not only the microstructure of the rose petal but also its minute nanostructures. The resulting PDMS replica (Figurs 3E,F) shows good replication quality for both micro- and nanosized surface features of the native petal.

The color of the petal is produced both in chemical and structural ways, which are defined as “chemical color”

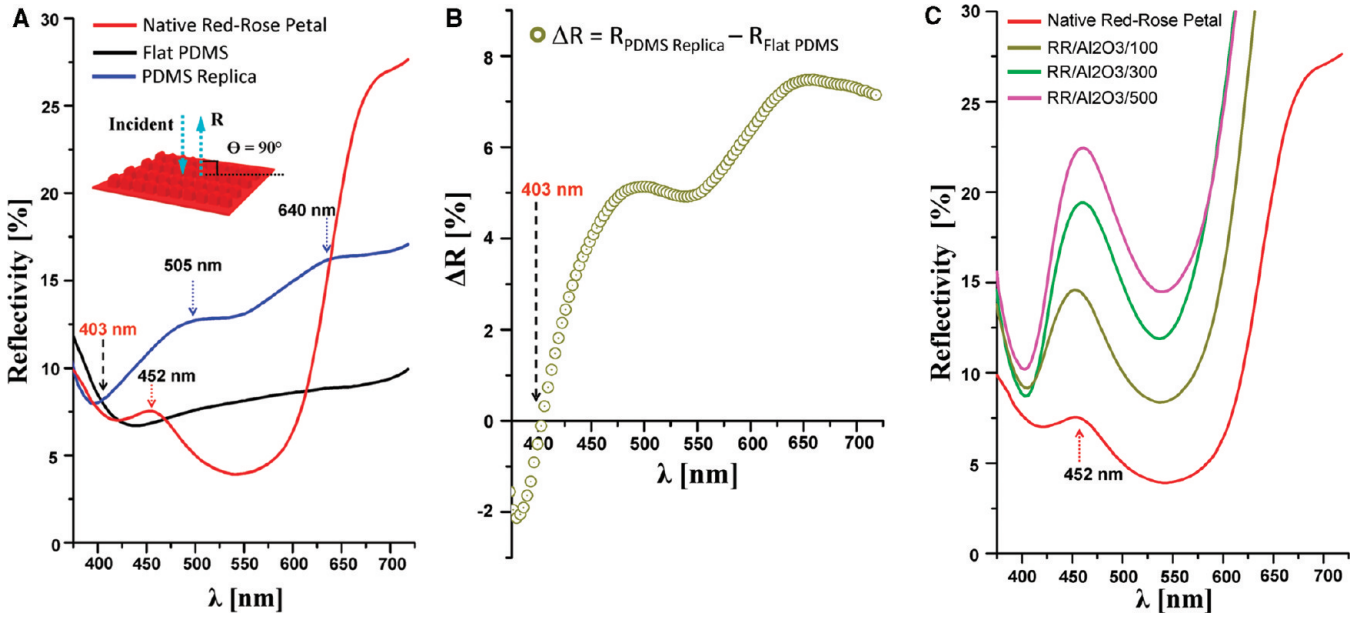

FIGURE 4. Reflectivity of a petal and its replica for normal angle of incidence. (A) Comparison of the absolute reflectivity of the native red-rose petal, the PDMS replica and the flat PDMS. (B) Absolute reflectivity difference (Δ*R*) between the PDMS replica and flat PDMS. (C) Comparison of the absolute reflectivity of the red-rose petal and Al_2O_3 coated red-rose petals with varying Al_2O_3 coating thicknesses. The increase of the feature size leads to shifts of the peak at 452 nm as a function of the coating thickness.

driven by pigments and "structural color" driven by the micro and nanosized minute structures, respectively (6, 12, 22). The chemical color of red flower petals is determined by a combination of anthocyanin and carotenoid pigments (23, 24). A precise determination of the particularly involved pigments is very difficult as the number of genetic variations of roses steadily grows, with currently more than 50 000 varieties having slightly different coloration. The visible appearance is strongly influenced by the varying mixture of pigments (23). The drying of the petals and the resulting dehydration of the pigments might also play a role for the visible appearance. Dehydrated pigments are known to change their color, which can be easily observed from dried flower petals. The dehydration is a continuous process, gradually changing the optical properties of the petals with time. In our case, we dried the petals in air in order to obtain a stable reference sample, although in this case, the pigments change their optical properties to a certain extent.

The cells placed on top of the petal surface are responsible for both the structural and chemical coloring effect. Those define the structure, but also contain the pigments, which are responsible for the chemical color (25). Therefore, a precise discrimination of the contribution of those two color effects to the resulting color is not straightforward. Figure 4A shows that the reflectance spectrum of a flat PDMS without micro- and nanosized surface structures exhibits a rather smooth and slow change in a broad wavelength range. In the wavelength region of 460−620 nm, the overall reflectance of the polymer is higher than of the native rose petal, which can be considered as an inherent optical reflectance behavior of pure PDMS. The reflectance of the native red-rose petal shows a minimum value at around 550 nm with a broad dip and rapidly increases for larger wavelengths. At a wavelength of around 452 nm, the reflectance of the rose petal has a local maximum. In the case of the PDMS replica without any pigmentation, the reflectance spectrum is strongly differing from the spectra of both the native red-rose petal and the flat PDMS. A comparison of the spectra of the flat PDMS and the PDMS replica shows a crossing point around 403 nm with a lower reflectance of the replica below that value and a higher reflectance above (Figure 4B), although the overall reflectance values in the entire wavelength region do not show significant differences. Notably, two features were detected in the vicinity of 505 and 640 nm, but a steep reflectance increase above 600 nm, which was observed from the native red-rose petal case, did not occur. The two features can be assigned to structure-based coloring effects caused by the hierarchical micro/nano surface structures of the red-rose petal, which were replicated in the PDMS. The reflecting behavior of the PDMS replica observed at 505 nm presumably corresponds to the behavior of the native rose-petal observed at 456 nm, with a slight shift in the wavelength. The shift might be caused by size deviations in the replicated minute structures compared to the native structures. As mentioned above, the sputtered Au layer and the nickel electroforming process may result in the structure sizes of the negative nickel replica becoming larger than those of the native petal, eventually leading to enlarged structure sizes of the resulting PDMS replica. Indeed, Figure 3 indicates that the replicated micro/nanostructures in the PDMS replica are larger than the native petal surface structures.

In order to validate the effects of the structure size on the reflectivity of the petal, we coated red-rose petal samples with amorphous Al_2O_3 (almost transparent in the visible range like PDMS) with varying thicknesses by ALD. The growth rate of the Al_2O_3 was around 1 Å/cycle. For instance, in the case of sample RR/Al2O3/500, the native petal was processed with 500 cycles, resulting in an Al_2O_3 coating with a thickness of around 50 nm. Similar to the reflectance

behavior of the PDMS replica, Al_2O_3 coated petals also show a slight position shift at 452 nm (Figure 4C). With increasing Al_2O_3 thickness, the peak (at 452 nm) is shifted to longer wavelengths accompanying an increase of reflectance. Although the exact origin of the shift at 454 nm is still unclear, it appears to be a unique feature caused by the slight size variation of the minute structures, as reported by Gaillot et al. (26). The shape of the peak noticeably becomes wider. The broad dip (around 530 nm) changes to a sharper shape, together with a reflectance increase. Although the light penetration/absorption depth into Al_2O_3 and the petal is not precisely determined with respect to the different wavelengths, this shape evolution is believed to indicate a weakening of the pigment effect and a strengthening of the structure effect with an increasing Al_2O_3 layer thickness. Consequently, we conclude that the size of the minute surface structures is a critical function to determine the reflectance of the replica (26, 27). By changing the structure size of the native petal surface, the reflecting behavior can be effectively modulated.

CONCLUDING REMARKS

From the optical reflectance measurement of the native rose petal and its positive PDMS replica made with a biotemplated two-step replication approach, we showed that the reflectance of PDMS can be easily modulated and an optical filtering effect can be induced in wavelengths around 403 nm. The reason for the optical behavior is the introduction of the red-rose petal's structural hierarchy into the polymer, separating the structure-induced reflectivity from the pigment-induced one. More notably, the reflectance of the petal was observed to significantly change with the size variation of the micro and nano structures present on the petal surface. The feature sizes were tuned with thin films of alumina deposited by atomic layer deposition. Furthermore, the structure-induced color appears attractive for some insects, which was also shown by Whitney et al. (5). We made a similar observation, namely that insects sometimes accumulated around the replica. These results could give useful information for the design of biomimetic optical devices, which are strongly related to the structure-based color and recently have been extensively studied (28).

Acknowledgment. This article is dedicated to the late Professor Ulrich Gösele and the late Professor Tai Hun Kwon. This work has received financial support from the German Federal Ministry of Education and Research (BMBF, FKZ 03X5507).

REFERENCES AND NOTES

(1) Koch, K.; Bhushan, B.; Barthlott, W. *Prog. Mater. Sci.* **2009**, *54*, 137–178.
(2) Koch, K.; Bhushan, B.; Barthlott, W. *Soft Mater.* **2008**, *4*, 1943–1963.
(3) Martens, P. *C. R. Acad. Sci. Paris* **1933**, *197*, 785–787.
(4) Feng, L.; Zhang, Y.; Xi, J.; Zhu, Y.; Wang, N.; Xia, F.; Jiang, L. *Langmuir* **2008**, *24*, 4114–4119.
(5) Whitney, H. M.; Kolle, M.; Andrew, P.; Chittka, L.; Steiner, U.; Glover, B. J. *Science* **2009**, *323*, 130–133.
(6) Glover, B. J.; Whitney, H. M. *Ann. Bot.* **2010**, *105*, 505–511.
(7) Denton, E. J. *Sci. Am.* **1971**, *224*, 64–72.
(8) Shawkey, M. D.; Estest, A. M.; Siefferman, L. M.; Hill, G. E. *Proc. R. Soc. London, B* **2003**, *270*, 1455–1460.
(9) Zi, J.; Yu, X.; Li, Y.; Hu, X.; Xu, C.; Wang, X.; Liu, X.; Fu, R. *Proc. Natl. Acad. Sci. U. S. A.* **2003**, *100*, 12576–12578.
(10) McClendon, J. H. *Am. J. Bot.* **1984**, *71*, 1391–1397.
(11) Lee, D. W. *Nature* **1991**, *349*, 260–262.
(12) Mason, C. W. *J. Phys. Chem.* **1927**, *31*, 1856–1872.
(13) Morrison, R. L. *Pigment Cell. Res.* **1995**, *8*, 28–36.
(14) Schulte, A. J.; Koch, K.; Spaeth, M.; Barthlott, W. *Acta Biomater.* **2009**, *5*, 1848–1854.
(15) Schweikart, A.; Zimin, D.; Handge, U. A.; Bennemann, M.; Altstädt, V.; Fery, A.; Koch, K. *Macromol. Chem. Phys.* **2010**, *211*, 259–264.
(16) Huang, J.; Wang, X.; Wang, Z. L. *Nano Lett.* **2006**, *6*, 2325–2331.
(17) Lee, S.-M.; Kwon, T. H. *Nanotechnology* **2006**, *17*, 3189–3196.
(18) Thangawng, A. L.; Ruoff, R. S.; Swartz, M. A.; Glucksberg, M. R. *Biomed. Microdevices* **2007**, *9*, 587–595.
(19) Being a line-of-sight deposition technique, sputtering can not deposit very uniform Au layer on a complicated 3D structure. Shadowed parts of the structure could not be coated well and thus Au-free regions could occur. Because of the existence of the Au-free regions, some parts of the biotemplates' surface could either be attacked by the electrolyte (assuming that an attack takes place rapidly) or a nickel deposition during electroforming might give inaccurate replication.
(20) Peuker, M. *Appl. Phys. Lett.* **2001**, *78*, 2208–2210.
(21) Hambach, D.; Schneider, G. *J. Vac. Sci. Technol., B* **1999**, *17*, 3212–3216.
(22) Kinoshita, S.; Yoshioka, S. *ChemPhysChem* **2005**, *6*, 1442–1459.
(23) Eugster, C. H.; Märki-Fischer, E. *Angew. Chem., Int. Ed.* **1991**, *30*, 654–672.
(24) Biolley, J. P.; Jay, M. *J. Exp. Bot.* **1993**, *44*, 1725–1734.
(25) Ozawa, A.; Uehara, T.; Sekiguchi, F.; Imai, H. *Opt. Rev.* **2009**, *16*, 458–460.
(26) Gaillot, D. P.; Deparis, O.; Welch, V.; Wagner, B. K.; Vigneron, J. P.; Summers, C. J. *Phys. Rev. E* **2008**, *78*, 031922.
(27) Feng, L.; Zhang, Y.; Li, M.; Zheng, Y.; Shen, W.; Jiang, L. *Langmuir* **2010**, *26*, 14885–14888.
(28) Vukusic, P.; Sambles, J. R. *Nature* **2003**, *424*, 852–855.

AM1007968